Microscopic Particle Motions in Strongly Coupled Dusty Plasmas

Lin I,* Wen-Tau Juan, Chih-Hui Chiang, J. H. Chu

The microscopic particle motions from the crystal to the disordered state of a dusty plasma with micrometer-sized silicon dioxide particle suspensions in a radio-frequency glow discharge system were studied through an optical microimaging system. Small-amplitude random motion around the lattice sites of the crystal state, relative domain motion with varying boundaries, cooperative hopping in the liquid state, and highly disordered motion with increasing radio-frequency power were observed. Chaotic states with different spatial scales under the coherent and stochastic coupling between dust particles and self-organized background plasma fluctuations were also demonstrated.

In a multiple-particle Coulomb system, the competition between the order caused by mutual Coulomb interactions and the disorder caused by random thermal motion of charged particles leads to different states ranging from solid crystals to liquids and plasmas (*1*). Named after the person who first studied it, the crystalline phase of such a system is known as a Wigner crystal (*1*), the structure and phase transitions of which have attracted sustained attention in the past several decades (*2*). However, the microscopic dynamic behaviors of Wigner crystals remain poorly understood because direct observation of the atomic scale systems that exist naturally is difficult. The search for a controllable and observable laboratory system is therefore important. After the theoretical prediction of dusty plasma crystals by Ikezi (*3*), the formation of crystals (*4–7*), liquids, and density waves (*5, 8*) in dusty plasma systems was demonstrated with simple optical microscopy.

Dusty plasma is a system consisting of fine dust particles suspended in a gaseous plasma background of electrons and ions. It exists widely in space and astroplasma systems and in laboratory plasma systems for fabricating materials (*9*). Because electrons have a higher mobility than do ions, a micrometer-sized dust particle in a plasma can carry thousands of electrons (*9*). This increases enormously the strength of Coulomb coupling between the dust particles and enables the formation of Coulomb crystals even at room temperature and submillimeter interparticle spacing.

This system can be viewed as a bridge connecting a condensed-matter system and a plasma system. In addition to being subjected to the strong interparticle forces that cause the formation of ordered structures and excitations, the motion of the dust particles is also coupled to the background plasma, which is well known to support many waves and low-dimensional chaos (*10*). On one hand, this coupling allows the efficient heating of the translational degree of dust particles through the background electric field fluctuations and provides a convenient and fast control of the melting process of dusty plasma crystals. This control opens a window to study generic behaviors of various crystal structures and phase transitions. On the other hand, the coupling is predicted to change the nature of the collective excitations of the background plasma itself (*10, 11*). By inducing an array of complex phenomena, dusty plasma broadens the scope of ordinary plasma as an arena for individual and nonlinear collective behaviors. We report the observation of several such phenomena and their particle motions: small-amplitude motions in the crystal state, domain motion with a finite lifetime around melting, collective and disordered motions, and heating in the liquid state induced by the coupling between particle motions and self-organized background plasma fluctuations.

The experiment was conducted in an annular radio-frequency (rf) dusty plasma trap described elsewhere (*4*). Micrometer-sized SiO_2 particles were generated through gas-phase reaction and aggregation by introducing O_2 and SiH_4 gases into the low-pressure rf Ar discharge and were confined in an annular plasma trap. The degree of Coulomb coupling decreases monotonically with increasing rf power, which in turn increases background plasma fluctuations. Particle motion was monitored with a digital video recording system through an optical microscope. In this study, we started from the hexagonal state. For this quasi–two-dimensional (2D) system, particle motion remains only on the horizontal focus

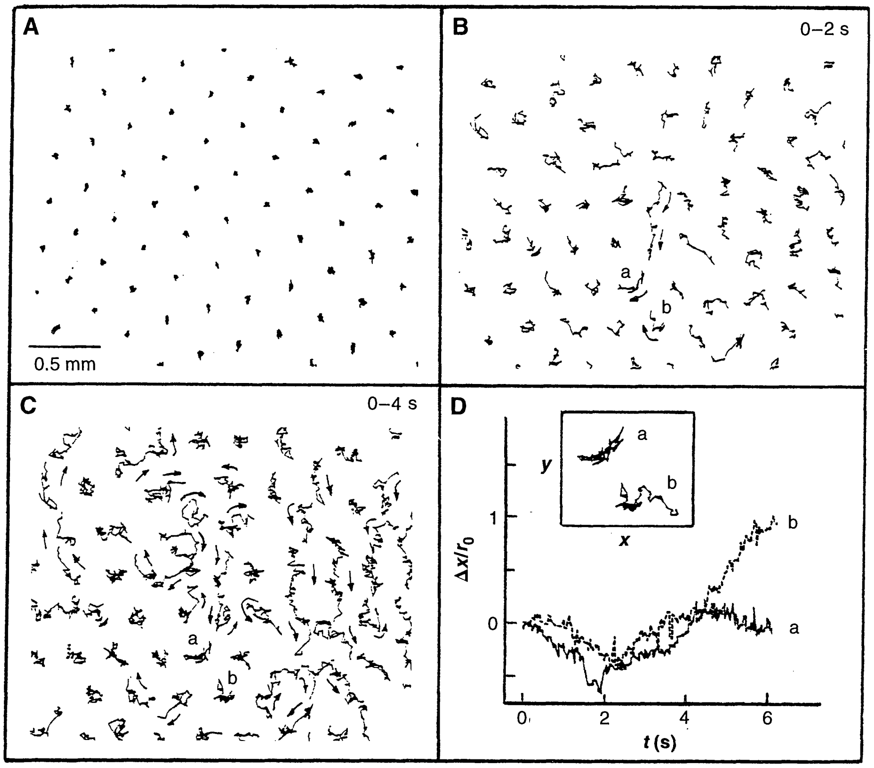

Fig. 1. (**A**) Trajectories of the hexagonal state (5-s exposure time, 15-Hz sampling rate, and about 200-μm mean particle separation). (**B** and **C**) Evolution of a typical liquid state with 15-Hz CCD (charge-coupled device) frame rate. The arrows indicate the direction of motion. (**D**) Partially correlated displacement normalized by the mean particle distance (r_0) of a pair of adjacent particles [particles a and b as shown in (B) and (C)].

Department of Physics, National Central University, Chungli, Taiwan 32054, Republic of China.

*To whom correspondence should be addressed.

plane in the crystal and cold liquid states and can be easily monitored. Why the hexagonal structure can be stable is an interesting issue but is not addressed in this paper.

The typical trajectories of particles, with small displacements around the equilibrium sites of the crystal in the 200-mtorr Ar plasma, are shown (Fig. 1A). In the liquid state, the long-range ordering is lost but the adjacent particle pairs are still partially correlated. The evolution of a typical liquid state is shown in Fig. 1, B (0 to 2 s) and C (0 to 4 s). Particles show large displacements and cooperative hopping (for example, the chain like hopping in the upper left corner of Fig. 1C). The typical partially correlated displacement from the initial position along the x axis of a pair of adjacent particles (particles a and b in Fig. 1C) is shown in Fig. 1D. Particle b suddenly hops to the right after the fourth second.

The sequential evolution of the microscopic state under a fixed rf power around melting is shown (Fig. 2). In general, collective excitation of ordered domains of different sizes and relative shear motions is observed. Some of these domains are rotational and some are stationary. For example, initially (Fig. 2A) the particles of the domain at the upper left corner rotate in a clockwise manner, with the particles around the domain boundary moving faster. The particles outside the domain boundary (those across the dashed line) move in the opposite direction. This crossover distorts the lattice and induces strong shear. As time passes, the domain boundary varies and the domain size fluctuates through the adjustment of local particle positions. The stationary particles can become mobile as time passes (see, for example, Fig. 2B for the next 15 s). The continuous excitation and relaxation processes limit domain lifetimes to several seconds in which the particles typically move collectively less than one lattice constant. The system runs through different microstates with different degrees of order and domain scales. Sometimes small vortices with diameters of about one or two lattice constants can be excited (Fig. 2D) as a result of the cyclic hopping. These vortices are similar to those found in computer simulations for other strongly coupled 2D systems (*12*). The small ring-shaped hopping around a center particle in Fig. 2D stops after one hop for each particle. Sometimes the system can enter a state with longer spatial correlations (Fig. 2C) or even reenter the highly ordered state similar to that shown in Fig. 1A but only with a lifetime of a few seconds (the good crystal state far below melting in Fig. 1A can last a few minutes).

The thermal excitation of domains with relative motion generates strong shear, distorts the lattice, and generates defects. This state is similar to the hexatic state predicted by the KTHNY theory (*13*), which gradually loses its translational order in the two-stage melting process of a 2D hexagonal lattice. Free dislocation and disclination defects have been observed in our system. Interesting dynamic processes such as generation, dissociation, propagation, recombination, and annihilation of free dislocations will be reported elsewhere.

Radio-frequency discharge is an open, nonlinear system. Even in the absence of particles, the stationary rf discharge alone exhibits self-organized order to spatiotemporal disorder behavior as the rf power increases (*10*). The liquid state of particles can also couple with the background plasma and induce self-organized long-wavelength fluctuations (*8*). The particle trajectories are superpositions of the random motions of the liquid and the collective motions. Two typical snapshots, each with a 15-ms exposure time

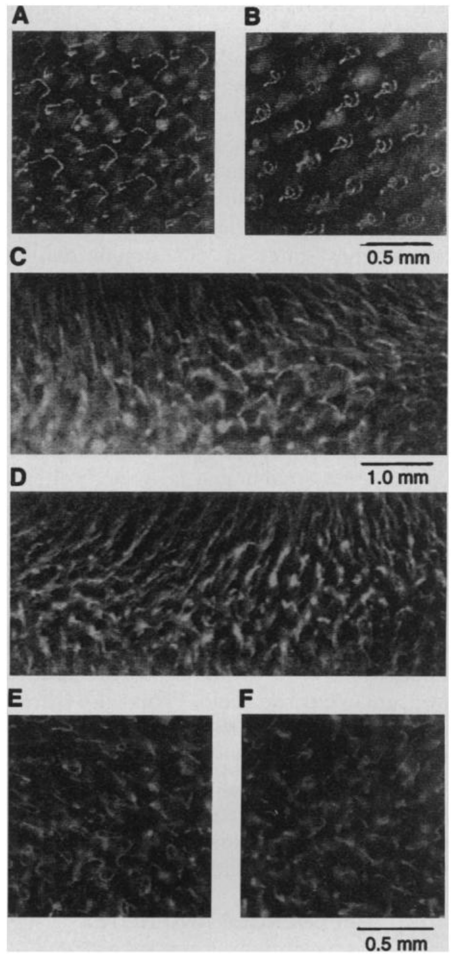

Fig. 3. (**A** and **B**) Two snapshots showing the typical temporally chaotic motion of the liquid state under self-organized long-wavelength excitation. (**C** and **D**) Sequential snapshots showing the chaotic motion with a spatial scale of a few millimeters. (**E** and **F**) Sequential snapshots showing the highly disordered motion under the stochastic coupling with the background fluctuation. The exposure time and CCD frame rate are 15 ms and 30 Hz, respectively.

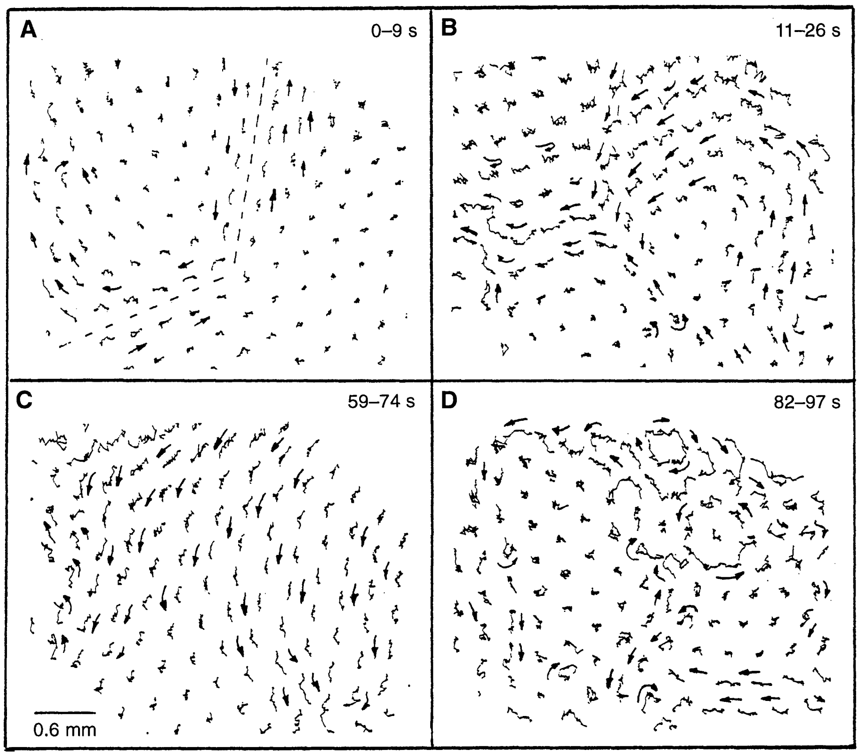

Fig. 2. (**A** through **D**) The evolution of the state around melting under a fixed control condition (3.3-Hz frame rate for the trajectories).

(Fig. 3, A and B), show that in a narrow rf power window all the particles in the same picture have the same temporally chaotic motion and similar interparticle distances.

At higher rf powers, a more chaotic 3D collective excitation with typical frequencies from 10 to 20 Hz and a length scale of a few millimeters (Fig. 3, C and D) is observed. The fluctuations of particle velocity and density are associated with the fluctuations in the local plasma emission (the emission from the atoms excited by electron impact collisions), which is a function of electron density (*8*). Another typical state exhibits disordered motion (Fig. 3, E and F). In this state, the contribution from the long-wavelength coherent part is much weaker than those in Fig. 3, C and D. Note that in all the pictures of Fig. 3, the particle speeds (>2 cm/s) are much higher than those in the liquid state shown in Fig. 1B. The corresponding kinetic energies (for a particle with a 5-μm diameter, 1 cm/s corresponds to about 5 eV kinetic energy) are many orders of magnitude higher than that supplied by the background neutral gas, which is at room temperature.

The rf dusty plasma system is a typical stationary, nonequilibrium open system with finite boundaries. Nevertheless, the low energy states of our system exhibit hexatic phase and rotational cooperative motions with various scales similar to other 2D thermal systems (*12–14*). Our first observations of the coherent and chaotic couplings between dust particles and self-organized background plasma fluctuations are the interesting and unique features of this open system attributable to its high energy and less viscous low-pressure background. Note that although dust particles are unlikely to gain energy from electron collisions because of large differences in mass, they can coherently or stochastically gain large amounts of energy (>10 eV) from fluctuations of a few millivolts in the low-frequency electric field. This also shows that, in addition to the general interest in its crystal structure, phase transition, and dusty plasma waves, dusty plasma is a good system in which to study nonlinear wave-particle interactions and heavy-particle motion in a chaotic background (*15*).

REFERENCES AND NOTES

1. E. Wigner, *Trans. Faraday Soc.* **34**, 678 (1939).
2. S. Ichimaru, *Rev. Mod. Phys.* **54**, 1017 (1982).
3. H. Ikezi, *Phys. Fluids* **29**, 1764 (1986).
4. J. H. Chu and Lin I, *Physica A* **205**, 183 (1994).
5. ______, *Phys. Rev. Lett.* **72**, 4009 (1994).
6. Y. Hayshi and K. Tachibana, *Jpn. J. Appl. Phys.* **33**, 804 (1994).
7. H. Thomas *et al.*, *Phys. Rev. Lett.* **73**, 625 (1994).
8. J. H. Chu, J. B. Du, Lin I, *J. Phys. D* **27**, 296 (1994); Lin I, C. S. Chern, J. H. Chu, J. M. Liu, J. B. Du, *Physica A* **205**, 443 (1994).
9. C. K. Goertz, *Rev. Geophys.* **27**, 271 (1989).
10. J. H. Chu and Lin I, *Phys. Rev. A* **39**, 233 (1989); Lin I and J. M. Liu, *Phys. Rev. Lett.* **74**, 3161 (1995).
11. R. K. Varma, P. K. Shulka, V. Krishan, *Phys. Rev. E* **47**, 3612 (1993).
12. P. Choquard and J. Clerouin, *Phys. Rev. Lett.* **50**, 2086 (1983); M. M. Hurley and P. Harrowell, *Phys. Rev. E* **52**, 1694 (1995); V. A. Schweigert and F. M. Peeters, *Phys. Rev. B* **51**, 7700 (1995).
13. J. M. Kosterlitz and D. J. Thouless, *J. Phys. C* **6**, 1181 (1973); A. P. Young, *Phys. Rev. B* **19**, 1855 (1979); B. I. Halperin and D. R. Nelson, *Phys. Rev. Lett.* **41**, 121 (1978).
14. See, for example, K. J. Strandburg, Ed., *Bond-Orientational Order in Condensed Matter Systems* (Springer, New York, 1992).
15. C. Jarzynski, *Phys. Rev. Lett.* **74**, 2937 (1995).

16. This work was supported by the Department of Physics, National Central University, and the National Science Council under contract NSC-85-2112-M008-011.

24 January 1996; accepted 18 April 1996

Electrical Properties of the Venus Surface from Bistatic Radar Observations

Gordon H. Pettengill,* Peter G. Ford, Richard A. Simpson

A bistatic radar experiment in 1994, involving reception on Earth of a specularly reflected, linearly polarized 13-centimeter-wavelength signal transmitted from the Magellan spacecraft in orbit around Venus, has established that the surface materials viewed at low and intermediate altitudes on Venus have a relative dielectric permittivity of 4.0 ± 0.5. However, bistatic results for the Maxwell Montes highlands imply an electrically lossy surface with an imaginary dielectric permittivity of $-i$ 100 ± 50, probably associated with a specific conductivity of about 13 mhos per meter. Candidates for highlands surface composition include ferroelectrics, a thin frost of elemental tellurium, or a plating of magnetite or pyrites.

Radio observations of the Venus highlands have revealed a surface material that exhibits radiothermal emissivity as low as 0.3 and normal-incidence radar reflectivity as high as 0.6 (*1, 2*). These values are not characteristic of most of the Venus surface, for which the emissivity is about 0.85 and the reflectivity is about 0.15 (*2*). The abrupt change in emissivity and reflectivity in the highlands occurs above an altitude of about 6054 km near the equator, increasing to above 6055.5 km at high northern latitudes. Mechanisms proposed to explain this unexpected behavior include scattering and emission from a roughened high-dielectric interface (*2*) and low-loss volume scattering from within the surface (*3*). As more observations have accumulated, it has become difficult to find appropriate materials that can satisfy all the known constraints of the scattering models.

Bistatic radar observations, in which the transmitter and receiver are physically separated and thus view the surface from different directions, can yield more information on the scattering process than can the usual backscattering geometry, particularly if a full polarization description of the echo is available (*4*). Bistatic radar observation of Venus requires a spacecraft because the maximum angular separation of Earth-based transmitters and receivers as viewed from Venus is less than 1 minute of arc. We were fortunate that the Magellan spacecraft (*5*), in orbit around Venus since August 1990, became available for such observations in late 1993, as it concluded its primary mission objectives.

Constrained by the distance to Venus (1.3 astronomical units) and by the relatively low radiated power available from Magellan (Table 1), we restricted the observations to a geometry in which the incident and emerging ray directions lay in the same vertical plane (the scattering plane) and made equal angles to the surface, taking advantage of the scattering enhancement associated with specular reflection. Equally important was the applicability of the

G. H. Pettengill and P. G. Ford, Center for Space Research, Massachusetts Institute of Technology, Cambridge, MA 02139, USA.
R. A. Simpson, Center for Radar Astronomy, Stanford University, Stanford, CA 94305, USA.

*To whom correspondence should be addressed.

Table 1. Magellan bistatic radar characteristics.

Parameter	Value
Magellan spacecraft transmitter	
Frequency	2.298 GHz
Wavelength	13.05 cm
Polarization	Linear
CW power	5 W
Antenna gain (3.7-m diameter)	35.9 dB
Antenna beamwidth	2.1° by 2.5°
Earth receiver (DSN DSS63)	
Antenna gain (70-m diameter)	63.3 dB
System temperature (viewing Venus)	20 K
Polarization	Left-right circular